INORGANIC CHEMISTRY
FRONTIERS

RESEARCH ARTICLE

View Article Online
View Journal | View Issue

Cite this: *Inorg. Chem. Front.*, 2020, **7**, 4404

Electrochemical synthesis of carbon nano onions†‡

Yixuan Bian, Lu Liu, Di Liu, Zhiwei Zhu, Yuanhua Shao and Meixian Li *

Received 7th August 2020,
Accepted 21st September 2020

DOI: 10.1039/d0qi00950d

rsc.li/frontiers-inorganic

As an important class of carbon nanomaterials, carbon nano onions (CNOs) have attracted considerable interest in recent years due to their unique structures and properties. In this work, the electrochemical synthesis of CNOs (including hollow carbon nano onions (H-CNOs) and solid carbon nano onions (S-CNOs)) was achieved from simple aromatic compounds in acetonitrile on a platinum plate electrode by a multi-potential steps method. The electrolytic products on the platinum plate electrode were separated to obtain H-CNOs and S-CNOs by heating treatment, followed by ultrasonic and gradient centrifugation. The reaction mechanism was presumed to be involved with dehydrogenation oxidation and reductive dimerization, as well as cross-linking reactions. The obtained H-CNOs and S-CNOs were characterized by scanning electron microscopy, transmission electron microscopy and Raman spectroscopy. This work has provided a new approach to synthesize and separate S-CNOs and H-CNOs. The developed method does not require sophisticated equipment or high energy consumption. The obtained CNOs would be applicable to construct electrocatalysis and sensing interfaces.

Carbon nanomaterials have received a great deal of attention since the discovery of the C_{60} fullerene molecule in 1985. Following on, carbon nanotubes and graphene have aroused great research interest due to their peculiar structures and properties.[1–3] As another unique allotropic form of carbon, carbon nano onions (CNOs) were actually discovered in 1980 before these carbon nanomaterials. However, they have long been overshadowed by these more popular carbon nanomaterials.[4] In the last several years, CNOs have attracted a great deal of attention because they show unique properties different from the other carbon nanomaterials. CNOs are composed of multi-layered concentric graphitic shells resembling that of an onion.[5] CNOs can be classified into two types, including hollow carbon nano onions (H-CNOs) consisting of polyhedral shaped shells and solid carbon nano onions (S-CNOs), which were composed of fullerene concentric spherical core–shell structure. The diameters of H-CNOs are usually between 5 and 50 nm, and they have larger specific surface areas than the same sized S-CNOs.

The unique structures of CNOs determine their peculiar properties, resulting in their prospective applications. CNOs can be used as electrode materials and supercapacitors because of their good electrical conductivity and large specific surface area.[6–8] With good biocompatibility, CNOs can be widely applied in the field of biosensing and detection.[9–11] CNOs exhibit catalytic properties in oxidative dehydrogenation reactions and oxygen reduction reactions.[12] Heteroatom-doped CNOs can also improve electrocatalytic activity and reduce costs, and are expected to replace traditional Pt-based electrocatalysts.[13–15] They can also accommodate electrolyte ions and quickly release stored energy, showing great potential in hydrogen storage materials.[16] Furthermore, because of their low friction, high stability and strong mechanical properties, CNOs are highly desired as solid lubricants in tribology.[17]

Broad applications of CNOs are dependent on their synthesis. Nowadays, the synthesis of CNOs has been realized through different methods. The first method reported by Sumio Iijima was the discovery of spherical CNOs as a byproduct of the synthesized carbon black created in vacuum using a transmission electron microscope (TEM) in 1980.[4] This process has also been thoroughly reinvestigated by Daniel Ugarte in 1992, and a formation mechanism for the creation of spherical graphitic structures has been observed *in situ*.[18] Chemical vapor deposition has also been a viable method to obtain CNOs, but they are usually contaminated by some catalyst particles encapsulated in carbon cages.[16,19,20] However, it is an easy way to obtain CNOs encapsulated with catalyst par-

College of Chemistry and Molecular Engineering, Beijing National Laboratory for Molecular Sciences, Peking University, Beijing 100871, P. R. China.
E-mail: lmwx@pku.edu.cn

†In celebration of the 110th anniversary of the College of Chemistry and Molecular Engineering of Peking University.

‡Electronic supplementary information (ESI) available: Fig. S1–S6. See DOI: 10.1039/D0QI00950D

ticles as efficient catalysts. Sano *et al.* fabricated CNOs by arc discharge between two graphite rods submerged in deionized water without metallic catalysts.[21,22] However, the products were a mixture of impurities, including amorphous carbon, graphite fragments, and carbon nanotubes. Although the purification was relatively complicated, it was easy to functionalize the CNOs.[23] The thermal annealing of the nanodiamond synthesized relatively large amounts of CNOs. However, it seemed difficult to separate them from the original diamond source.[24–27] Detonation synthesis of CNOs *via* liquid carbon condensation has been also reported.[28] All in all, most of the methods mentioned above not only require high energy consumption, but also have a very low yield of CNOs with complex purification treatment. Moreover, different synthetic techniques could be used to produce CNOs with different structures and properties. So, the best way to choose a synthetic technique is based on the purpose of synthetic CNOs.

It is important to develop a simple and cheap method for the large-scale synthesis of high quality CNOs due to their potential applications. Thus, researchers have been exploring new synthetic techniques of CNOs. In recent years, curved nano-graphene, uniform carbon nanotubes and carbon nanoribbons have been synthesized using organic chemistry methods by Itami's research group.[29–31] These nanometre-sized carbon materials (abbreviated as nanocarbons) consisting of benzene units could be prepared by bottom-up construction from relatively simple aromatic compounds, involving the coupling, reductive dimerization and cyclodehydrogenation oxidation reactions. Compared with organic synthesis, electrochemical synthesis has many significant advantages. Electrochemical synthesis is performed through oxidation–reduction reactions in electrolytic cells.[32,33] As a clean reaction reagent, electrons avoid the use of dangerous oxidants and reducing agents. Furthermore, electron transfer and chemical reaction proceed at the same time. The reaction rate can be changed by controlling the potential to reduce side reactions. These advantages result in a high-purity product with an easy separation, and reduce environmental pollution. The reaction could also be carried out at room temperature and atmospheric pressure without the need for special heating and pressure equipment.

Considering the economics and convenience of electrochemical synthesis, we believe that the electrochemical synthesis of nanocarbons by dehydrogenation oxidation and reductive dimerization, as well as cross-linking reactions based on simple aromatic compounds, is possible by controlled-potential electrolysis. S-CNOs made directly from CO_2 by molten electrolysis have been reported,[34] but it needs high temperature. The electrochemical synthesis of CNOs-polypyrrole composites has also been studied.[35] In this work, we proposed a method for the synthesis and separation of S-CNOs and H-CNOs by electrolysis of toluene on platinum electrodes. The developed route is facile to obtain S-CNOs and H-CNOs at the same time, and overcomes some drawbacks discussed earlier. A simple purification process can completely remove byproducts, and separate the S-CNOs and H-CNOs in the products.

Experimental

Materials

Toluene, sulfuric acid and hydrogen peroxide (aqueous solution) were purchased from Xilong Chemical Co., Ltd. Acetonitrile was obtained from Thermo Fisher Scientific Co., Ltd. Tetrabutylammonium perchlorate (TBAP), benzene and 1,2-dimethylbenzene were ordered from Sigma-Aldrich. 1-Methylnaphthalene was purchased from Xingkeyuan Information Technology Co., Ltd *N*-cyclohexylpyrrolidone (CHP) was bought from Tianjin Sean Opde Technology Co., Ltd. All chemicals were of analytical grade and used without further purification.

Synthetic procedures

Electrochemical synthesis of CNOs. All electrochemical synthesis processes were carried out on a CHI 660D electrochemical workstation (Shanghai Chen-Hua, China) at room temperature in a glovebox (VG1200/750TS, Vigor, America) under a nitrogen atmosphere. Two identical platinum plate electrodes (30 × 30 × 0.1 mm) were used as the working electrode and the counter electrode. Before the electrochemical synthesis, the platinum electrodes were carefully cleaned with a mixture of concentrated sulfuric acid and 30% hydrogen peroxide (7 : 3), then rinsed with water and acetone successively, and dried by a blower. The silver wire coated with silver chloride (Ag/AgCl) was used as the quasi-reference electrode, and the tube with porous ceramic was used for preventing the introduction of silver nanoparticles in the system. In a typical procedure, CNOs were synthesized by multi-potential steps method in 30 mL of acetonitrile containing 5 mM toluene and 0.1 M TBAP in an electrolytic cell with a maximum capacity of 50 mL (Fig. S1‡). The step potential was from 2.2 V to −1.6 V (*vs.* Ag/AgCl), and the step time was 10 s.

Separation and purification. The electrolytic products stuck on the electrodes were collected and washed with acetonitrile, then heated to 450 °C in a muffle furnace with a ramp rate of 2 °C min^{-1}, and maintained for 3 hours. After natural cooling, the heat-treated mixed products were dispersed in CHP by ultrasound for 1 h, and centrifuged at each speed of 6000 rpm, 8000 rpm, 10 000 rpm, and 12 000 rpm for half an hour. The centrifuged products were collected and characterized by TEM.

Characterizations. TEM and energy-dispersive X-ray spectra (EDS) were studied by a JEM-2100F electron microscope (JEOL, Japan) at an acceleration voltage of 200 kV. Scanning transmission electron microscopy (STEM) images were obtained on a JEM-2100F electron microscope (JEOL, Japan). The Raman spectra were obtained *via* Raman spectrometer (DXRxi) by using a laser at 514 nm. Thermogravimetric analysis (TG) was performed using Q600 SDT at a ramp rate of 5 °C min^{-1} under air flow over a temperature range of 20–900 °C. Gas chromatography-mass spectrometry (GC-MS) was performed on a

Hybrid Quadrupole-Orbitrap GC-MS/MS System (Thermo Fisher Scientific, Italy). The injection port temperature was set to 280 °C, and the injection volume was set to 2 μL with a split ratio of 5 : 1. The compounds were separated on a 100% dimethylpolysiloxane column (Agilent, USA). He (99.9999%) was employed as carrier gas. The flow of the carrier gas was set to 1.0 mL min^{-1}. The temperature program was at 40 °C for 2 min, and then increased from 40 to 350 °C at 20 °C min^{-1}. The transfer line was set to 280 °C, and the ion source was set to 300 °C. Electron ionization was performed using an electron energy of 70 eV.

Results and discussion

The electrochemical properties of acetonitrile and toluene, with 0.1 M TBAP as the supporting electrolyte, were investigated on a platinum electrode (20 × 10 × 0.1 mm) under nitrogen atmosphere by cyclic voltammetry (CV) using a typical three-electrode system at 20 °C in a glovebox. As shown in Fig. 1, in the range of 2.4 V −1.8 V (*vs.* Ag/AgCl), the platinum plate electrode had almost no redox peak for acetonitrile (black line). After adding 5 mM toluene to the solution, the CV curves showed significant oxidation current from the start of about 1.8 V in the positive scan range from 0 to 2.4 V. Moreover, two reduction peaks appeared at −0.16 V and 0.07 V in the reverse scan. However, no obvious reduction peak could be observed in the negative scan from 0 to −2.0 V. These suggest that an irreversible oxidation occurred in toluene, and the oxidation product could be reduced in the reverse scan. Based on the previously reported work,[36,37] the electro-oxidation of toluene in organic media on the Pt electrode could form conducting polymer films. We presumed that CNOs might be produced from toluene by electrochemical polymerization.

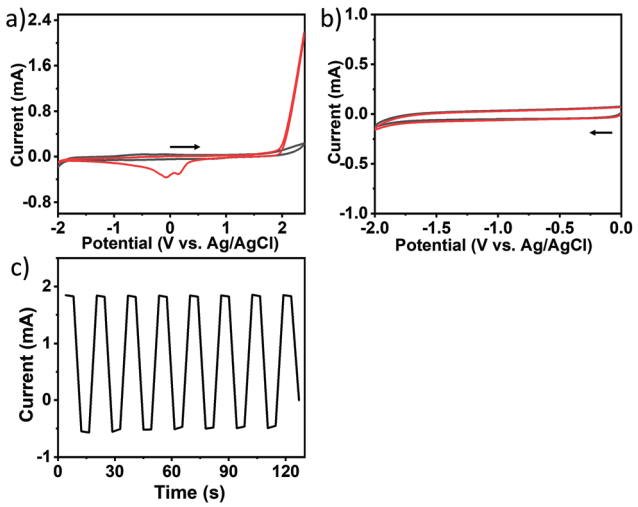

Fig. 1 (a) CV curves in acetonitrile (black line) and 5 mM toluene in acetonitrile (red line) with 0.1 M TBAP in a positive scan. (b) CV curves in acetonitrile (black line) and 5 mM toluene in acetonitrile (red line) with 0.1 M TBAP in a negative scan. The scan rates were all 50 mV s^{-1}. (c) Multi-potential steps chronoamperometric curves in a mixed solution of 5 mM toluene and acetonitrile containing 0.1 M TBAP with the step potential from 2.2 V for 10 s to −1.6 V for 10 s.

According to the CV plot, we tried to synthesize CNOs using different electrolysis methods. It was found that the Pt electrode was oxidized and reduced to produce large amounts of platinum nanoparticles by controlled-current electrolysis due to poor selectivity. If the controlled-potential electrolysis was employed at a relatively positive potential, for example 2.4 V in a divided cell for 24 hours, no CNOs were obtained by characterizations. So a multi-potential steps method was used to synthesize CNOs in an undivided cell at different potentials, taking an electrolysis step from 2.2 V for 10 s to −1.6 V for 10 s as an example, as shown in Fig. 1c. As electrolysis occurred, many bubbles were observed on the cathode, and they were hydrogen bubbles resulted from hydrogen ions by electro-oxidative dehydrogenation of toluene on the anode, following that brown liquid was formed to diffuse into the solution. As electrolysis process continued, the color of the solution gradually became darker. After electrolysis of about 10 hours, the solution was dark brown with brown precipitate, and black sheet-like products were attached on the working electrode.

The products on the electrode were collected, and then washed with acetonitrile to remove remained TBAP. TEM was employed to characterize the composition and morphology of the products dispersed in acetonitrile. Fig. S2‡ displayed that the products consisted of amorphous carbon, Pt NPs, S-CNOs and H-CNOs, moreover, S-CNOs and H-CNOs were apt to form aggregates on the carbon film, respectively, which indicated strong interaction of the same structural molecules. EDS characterization further verified the elemental composition of the mixed products include Pt, C, Cl and O, as shown in Fig. S3.‡ Among them, trace amounts of Cl and O might be from the supporting electrolyte TBAP and the substrate. An electrolytic solution after electrolysis of 5 hours was analyzed by GC-MS, some stable radicals and polycyclic aromatic hydrocarbons were identified such as C_6H_5 (phenyl), C_7H_7 (benzyl), C_9H_7 (indenyl), $C_{10}H_8$ (naphthalene), $C_{11}H_9$ (methyl-naphthyl radical), $C_{12}H_8$ (acenaphthylene and/or ethynylnaphthalene), $C_{13}H_9$ (fluorenyl and/or phenalene radicals), $C_{14}H_{10}$ (anthracene and/or phenanthrene), $C_{14}H_{14}$ (dimethylbiphenyl),[38] as shown in Fig. S4.‡ From the composition of electrolytic products, we presumed that the reaction mechanism might be involved with dehydrogenation oxidation of toluene generating benzyl radical cations and phenyl radical cations, which participate in the next reductive dimerization as well as cross-linking reactions to form polycyclic aromatic hydrocarbons during the processes of electro-oxidation and electro-reduction,[36,37] but conversion of polycyclic aromatic hydrocarbons to CNOs is unclear, which needs further study.

Due to the complex mixture, it is very important to explore the separation method for different components. To obtain the properties of different products, TG was employed to characterize the thermal stability of the mixed products from 20 to 900 °C with a heating rate of 5 °C min^{-1}. Fig. 2a shows that some compounds decomposed in the range from 100 °C

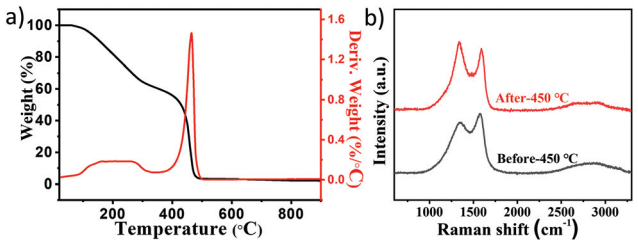

Fig. 2 (a) TG and DTG curves of the mixed product in the range of 20–900 °C under airflow. (b) Raman spectra of the mixed product before and after heated at 450 °C.

to 300 °C in air, and amorphous carbon started burning at about 400 °C based on the previously reported work.[39,40] Due to the stability of Pt NPs and CNOs, most of the amorphous carbon lost weight from 400 °C to 500 °C. Different temperature programs were tested to treat the products under air conditions in order to optimize the removal of amorphous carbon in the mixed products, and the results suggest that the impurities could be removed when the temperature was not below 450 °C (Fig. S5–7‡). However, in order to avoid the oxidation of CNOs at higher temperature, the amorphous carbon in the product was removed by heating at 450 °C for 3 hours.

The products before and after heat treatment were further characterized by Raman spectrometry. Fig. 2b shows the Raman spectra of the products. There were two broad Raman bands at around 1350 and 1569 cm^{-1} before heat treatment. The G band at about 1569 cm^{-1} corresponds to the E_{2g} mode in the graphite structure of carbon, and the D band appears at about 1350 cm^{-1} to characterize the disorder in sp^3 carbon materials. The relative intensity of the D to G bands (I_D/I_G) and the G band peak position could be used to represent the graphitization degree of the samples.[41] Because of this, the increases in the intensity ratio of I_D/I_G from 0.83 to 1.08 and the G band peak position from 1569 cm^{-1} to 1591 cm^{-1} were attributed to increased graphitic structure of the sample due to the removal of amorphous carbon after heat treatment. Moreover, the full widths at half-maximum (FWHM) of the G band and D band were narrowed, which means more order in the structure.[42–44]

Depending on the sizes of the different materials, the Pt NPs and two kinds of CNOs were separated by combination of sonication and gradient centrifugation after removing the amorphous carbon. The heat-treated products were ultrasonically dispersed in CHP for 1 h to form a black suspension at a concentration of 1 mg mL^{-1}. Unfortunately, the products could not be totally separated by gradient centrifugation because they could not be dispersed very well at this concentration (Fig. S6‡). A suspension with a concentration of 1 μg mL^{-1} in CHP was then prepared by sonication for 1 hour, followed by centrifugation at 6000 rpm for 30 min to remove Pt NPs. Next, the supernatant was centrifuged at 8000 rpm for 30 min and the precipitation was collected to obtain S-CNOs. At last, the remaining supernatant was centrifuged at 12 000 rpm for 30 min, and the obtained precipitation was H-CNOs. TEM characterization verified the separation of S-CNOs and H-CNOs, as shown in Fig. 3. The structure of the obtained

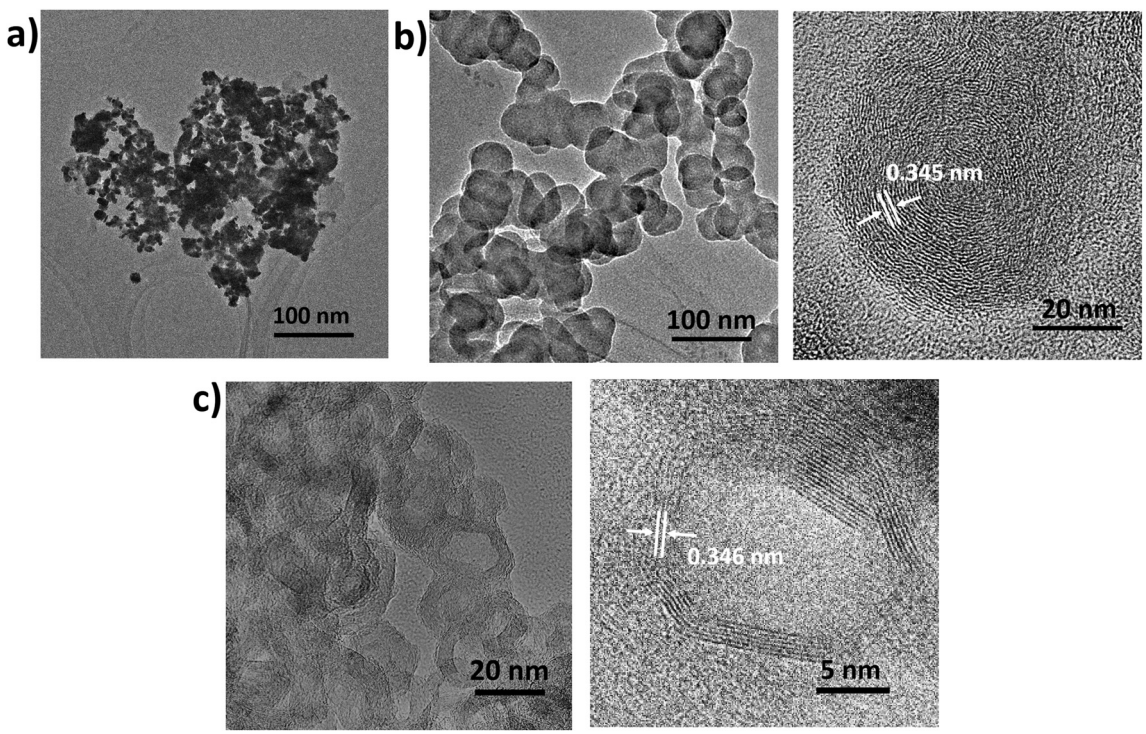

Fig. 3 TEM images of the collected products by ultrasonic dispersion in CHP for 1 h at a concentration of 1 μg mL^{-1}, and centrifugation at (a) 6000 rpm, (b) 8000 rpm and (c) 12 000 rpm.

single H-CNO particle was also investigated by TEM at different tilt angles of 0, 10, 30, and −50 degrees. As shown in Fig. 4, the sidewalls of the H-CNO particle got darker in color with increasing tilt angle, indicating that the areas of the sidewalls gradually increased. The color of the central domain of H-CNO is the same as that of the substrate, which illustrates that the H-CNO particle is a hollow structure. Further simulation of the contrast changes upon tilt angle for the hollow and core–shell particles was done. Only the hollow configuration matched the TEM observations, and the TEM images displayed a polyhedral shaped shell. The corresponding width at 10 degrees was 1.7 nm, and the right height was calculated to be about 9.7 nm. At 30 degrees, the width was 5 nm, and the right height was about 10 nm. At −50 degrees, the width was 7.5 nm and the left height was about 9.8 nm. These results proved that the H-CNOs have a hollow structure with a length of 27 nm, width of 17 nm, and height of 9.8 nm. STEM EDS mapping data showed that the H-CNOs and S-CNOs were made up of the element C. In addition, the element O existed as a composition of the substrate because its distribution was homogeneous (Fig. S9‡). These results suggest that H-CNOs and S-CNOs were hardly functionalized with oxygen after heating at 450 °C for three hours.

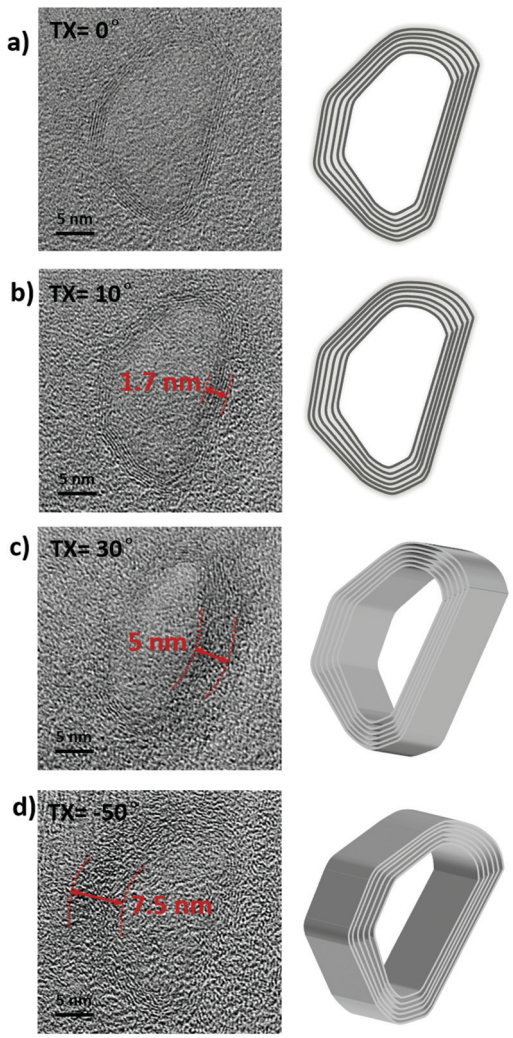

Fig. 4 TEM images and projection images of the polyhedral H-CNOs observed with tilting angles of (a) 0, (b) 10, (c) 30, and (d) −50 degrees.

The obtained H-CNOs and S-CNOs products were further studied by Raman spectrometry. They both showed strong and sharp G and D peaks, as shown in Fig. 5. This is similar to the nanodiamond-derived CNOs obtained by annealing detonation nanodiamond powders at 1650 °C under the flow of helium gas,[45,46] and suggests very small sizes. The 2D band at 2680 cm^{-1} and D + G band at 2920 cm^{-1} were attributed to the second-order two-phonon process and the combination of phonons with different momenta. These are activated by double resonance processes, and demonstrate the multi-layer graphite structure of CNOs and defects of CNOs.[47,48]

The effects of toluene concentration, and the step potential and step time used in the multi-potential steps method on the products were investigated to optimize the synthetic conditions. After electrolysis for 24 hours, the electrolytic product on the electrode surface under different conditions was collected and compared after proper separation. First, different concentrations of toluene were tested. It was found that a longer time was needed to form products on the electrode with increasing toluene concentration from 5 mM to 1.5 M. However, no more CNOs could be obtained. Therefore, 5 mM toluene was chosen as the synthetic condition. Secondly, different anode potentials were applied, including 1.6 V, 1.8 V, 2.0 V, 2.2 V and 2.4 V, at a fixed cathode potential of −1.8 V with a step time of 10 s. It was found that the electrodeposited loading on the electrode increased with the positive shifts of the anode potential. However, when the anode potential was fixed at 2.4 V, the amount of Pt NPs in the product increased and the working electrode was significantly oxidized. Therefore, 2.2 V was selected as the oxidation potential of the multi-potential steps method. Thirdly, different cathode potentials were tested. The reduction potential gradually changed to a more negative potential over continuous scanning due to the effect of the overpotential. Thus, in order to assure that the electro-reduction reaction of the electro-oxidative product could occur, relatively negative potentials at −1.0 V, −1.2 V, −1.4 V and −1.6 V were utilized. Similar results were obtained; that is, the amounts of the electrolytic product on the electrode clearly rose with the negative shifts of the cathode potential. Therefore, −1.6 V was selected as the reduction potential of the multi-potential steps method.

The effect of different step times with the multi-potential steps method was also studied. The results indicated that more electrolytic products were formed on the working electrode with increasing step time from 1 s to 10 s. Furthermore, the loading on the electrode increased more rapidly, and the ratio of amorphous carbon to CNOs gradually decreased. When the step time changed from 10 s to 50 s, the oxidation and reduction products diffused away from the electrode as the step time increased. This resulted in lower quantities of products on the electrode surface. Moreover, the ratio of amorphous carbon to CNOs gradually increased. So, the optimal

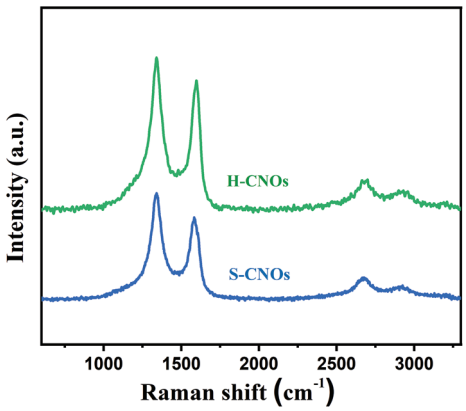

Fig. 5 Raman spectra of purified H-CNOs and S-CNOs.

electrolytic conditions for the synthesis of CNOs by multi-potential steps method were a step potential from 2.2 V to −1.6 V with a step time of 10 s. In the mean time, the other aromatic compounds (including benzene, 1,2-dimethylbenzene and 1-methylnaphthalene) were also tested. It was found that H-CNOs and S-CNOs could be obtained under proper conditions.

Conclusions

A one-step electrochemical synthetic route to obtain H-CNOs and S-CNOs has been developed. The synthetic route is based on a controlled-potential electrolysis method with the multi-potential steps in a mixed solution of toluene and acetonitrile containing 0.1 M TBAP on a Pt electrode. The possible reaction mechanism, which needs further study, might be involved with dehydrogenation oxidation and reductive dimerization, as well as cross-linking reactions. The obtained products comprise S-CNOs, H-CNOs, amorphous carbon and Pt NPs. Among them, amorphous carbon could be removed by heating in air, and Pt NPs could be abandoned by centrifugation. S-CNOs and H-CNOs have been totally separated by ultrasonic and gradient centrifugation. Our work has provided a new approach to synthesize and separate S-CNOs and H-CNOs. The developed method does not require sophisticated equipment. The obtained CNOs would be applicable to the construction of electrocatalysis and sensing interfaces.

Conflicts of interest

There are no conflicts to declare.

Acknowledgements

We appreciate the National Natural Science Foundation of China (no. 21974003 and 21675003) for financial support.

References

1 H. W. Kroto, J. R. Heath, S. C. O'Brien, R. F. Curl and R. E. Smalley, C60: Buckminsterfullerene, *Nature*, 1985, **318**, 162–163.
2 S. Iijima, Helical microtubules of graphitic carbon, *Nature*, 1991, **354**, 56–58.
3 K. S. Novoselov, A. K. Geim, S. V. Morozov, D. Jiang, Y. Zhang, S. V. Dubonos, I. V. Grigorieva and A. A. Firsov, Electric field effect in atomically thin carbon films, *Science*, 2004, **306**, 666–669.
4 S. Iijima, Direct observation of the tetrahedral bonding in graphitized carbon black by high resolution electron microscopy, *J. Cryst. Growth*, 1980, **50**, 675–683.
5 D. Ugarte, Onion-like graphitic particles, *Carbon*, 1995, **33**, 989–993.
6 V. K. A. Muniraj, C. K. Kamaja and M. V. Shelke, $RuO_2{\cdot}nH_2O$ nanoparticles anchored on carbon nano-onions: An efficient electrode for solid state flexible electrochemical supercapacitor, *ACS Sustainable Chem. Eng.*, 2016, **4**, 2528–2534.
7 C. Wang, C. Wu, S. Chen, Q. He, D. Liu, X. Zheng, Y. A. Haleem and L. Song, In situ synthesis of noble metal nanoparticles on onion-like carbon with enhanced electrochemical and supercapacitor performance, *RSC Adv.*, 2017, **7**, 4667–4670.
8 D. Mohapatra, G. Dhakal, M. S. Sayed, B. Subramanya, J. J. Shim and S. Parida, Sulfur doping: Unique strategy to improve the supercapacitive performance of carbon nano-onions, *ACS Appl. Mater. Interfaces*, 2019, **11**, 8040–8050.
9 M. Rizwan, M. Hazmi, S. A. Lim and M. U. Ahmed, A highly sensitive electrochemical detection of human chorionic gonadotropin on a carbon nano-onions/gold nanoparticles/polyethylene glycol nanocomposite modified glassy carbon electrode, *J. Electroanal. Chem.*, 2019, **833**, 462–470.
10 V. Sok and A. Fragoso, Amperometric biosensor for glyphosate based on the inhibition of tyrosinase conjugated to carbon nano-onions in a chitosan matrix on a screen-printed electrode, *Mikrochim. Acta*, 2019, **186**, 569.
11 J. C. Zuaznabar-Gardona and A. Fragoso, Development of highly sensitive IgA immunosensors based on co-electropolymerized L-DOPA/dopamine carbon nano-onion modified electrodes, *Biosens. Bioelectron.*, 2019, **141**, 111357.
12 K. Khan, A. K. Tareen, M. Aslam, Y. Zhang, R. Wang, S. A. Khan, Q. U. Khan, M. Rauf, H. Zhang, Z. Ouyang and Z. Guo, Facile synthesis of mayenite electride nanoparticles encapsulated in graphitic shells like carbon nano onions: Non-noble-metal electrocatalysts for oxygen reduction reaction (ORR), *Front. Chem.*, 2019, **7**, 934.
13 K. Chatterjee, M. Ashokkumar, H. Gullapalli, Y. Gong, R. Vajtai, P. Thanikaivelan and P. M. Ajayan, Nitrogen-rich carbon nano-onions for oxygen reduction reaction, *Carbon*, 2018, **130**, 645–651.
14 T. H. Han, D. Mohapatra, N. Mahato, S. Parida, J. H. Shim, A. T. N. Nguyen, V. Q. Nguyen, M. H. Cho and J.-J. Shim,

Effect of nitrogen doping on the catalytic activity of carbon nano-onions for the oxygen reduction reaction in microbial fuel cells, *J. Ind. Eng. Chem.*, 2020, **81**, 269–277.

15 Y. Zhang, A. Reed and D. Y. Kim, Nitrogen doped carbon nano-onions as efficient and robust electrocatalysts for oxygen reduction reactions, *Curr. Appl. Phys.*, 2018, **18**, 417–423.

16 C. Zhang, J. Li, E. Liu, C. He, C. Shi, X. Du, R. H. Hauge and N. Zhao, Synthesis of hollow carbon nano-onions and their use for electrochemical hydrogen storage, *Carbon*, 2012, **50**, 3513–3521.

17 L. Ning, X. X. Jun, S. Tao, L. L. Han and X. Sun, One-step gas-liquid detonation synthesis of carbon nano-onions and their tribological performance as lubricant additives, *Diamond Relat. Mater.*, 2019, **97**, 107448.

18 D. Ugarte, Curling and closure of graphitic networks under electron-beam irradiation, *Nature*, 1992, **359**, 707.

19 C. He, N. Zhao, C. Shi, X. Du and J. Li, Carbon nanotubes and onions from methane decomposition using Ni/Al catalysts, *Mater. Chem. Phys.*, 2006, **97**, 109–115.

20 X. Xu, G. Wang, G. Wan, S. Shi, C. Hao, Y. Tang and G. Wang, Magnetic Ni/graphene connected with conductive carbon nano-onions or nanotubes by atomic layer deposition for lightweight and low-frequency microwave absorption, *Chem. Eng. J.*, 2020, **382**, 122980.

21 N. Sano, H. Wang, I. Alexandrou, M. Chhowalla, K. B. K. Teo, G. A. J. Amaratunga and K. Iimura, Properties of carbon onions produced by an arc discharge in water, *J. Appl. Phys.*, 2002, **92**, 2783–2788.

22 N. Sano, H. Wang, M. Chhowalla, I. Alexandrou and G. A. J. Amaratunga, Synthesis of carbon onions in water, *Nature*, 2001, **414**, 506–507.

23 A. S. Rettenbacher, B. Elliott, J. S. Hudson, A. Amirkhanian and L. Echegoyen, Preparation and functionalization of multilayer fullerenes (carbon nano-onions), *Chem. – Eur. J.*, 2006, **12**, 376–387.

24 Z. Feng, Y. Lin, C. Tian, H. Hu and D. Su, Combined study of the ground and excited states in the transformation of nanodiamonds into carbon onions by electron energy-loss spectroscopy, *Sci. Rep.*, 2019, **9**, 3784.

25 V. L. Kuznetsov, I. L. Zilberberg, Y. V. Butenko, A. L. Chuvilin and B. Segall, Theoretical study of the formation of closed curved graphite-like structures during annealing of diamond surface, *J. Appl. Phys.*, 1999, **86**, 863–870.

26 E. D. Obraztsova, M. Fujii, S. Hayashi, V. L. Kuznetsov, Y. V. Butenko and A. L. Chuvilin, Raman identification of onion-like carbon, *Carbon*, 1998, **36**, 821–826.

27 S. Tomita, T. Sakurai, H. Ohta, M. Fujii and S. Hayashi, Structure and electronic properties of carbon onions, *J. Chem. Phys.*, 2001, **114**, 7477–7482.

28 M. Bagge-Hansen, S. Bastea, J. A. Hammons, M. H. Nielsen, L. M. Lauderbach, R. L. Hodgin, P. Pagoria, C. May, S. Aloni, A. Jones, W. L. Shaw, E. V. Bukovsky, N. Sinclair, R. L. Gustavsen, E. B. Watkins, B. J. Jensen, D. M. Dattelbaum, M. A. Firestone, R. C. Huber, B. S. Ringstrand, J. R. I. Lee, T. van Buuren, L. E. Fried and T. M. Willey, Detonation synthesis of carbon nano-onions via liquid carbon condensation, *Nat. Commun.*, 2019, **10**, 3819.

29 H. Omachi, T. Nakayama, E. Takahashi, Y. Segawa and K. Itami, Initiation of carbon nanotube growth by well-defined carbon nanorings, *Nat. Chem.*, 2013, **5**, 572–576.

30 H. Omachi, Y. Segawa and K. Itami, Synthesis of cycloparaphenylenes and related carbon nanorings: a step toward the controlled synthesis of carbon nanotubes, *Acc. Chem. Res.*, 2012, **45**, 1378–1389.

31 Y. Segawa, A. Yagi, K. Matsui and K. Itami, Design and synthesis of carbon nanotube segments, *Angew. Chem., Int. Ed.*, 2016, **55**, 5136–5158.

32 A. Badalyan and S. S. Stahl, Cooperative electrocatalytic alcohol oxidation with electron-proton-transfer mediators, *Nature*, 2016, **535**, 406–410.

33 E. J. Horn, B. R. Rosen, Y. Chen, J. Tang, K. Chen, M. D. Eastgate and P. S. Baran, Scalable and sustainable electrochemical allylic C–H oxidation, *Nature*, 2016, **533**, 77–81.

34 X. Liu, J. Ren, G. Licht, X. Wang and S. Licht, Carbon dioxide mitigation: Carbon nano-onions made directly from CO_2 by molten electrolysis for greenhouse gas mitigation, *Adv. Sustainable Syst.*, 2019, **3**, 1970021.

35 O. Mykhailiv, M. Imierska, M. Petelczyc, L. Echegoyen and M. E. Plonska-Brzezinska, Chemical versus electrochemical synthesis of carbon nano-onion/polypyrrole composites for supercapacitor electrodes, *Chem. – Eur. J.*, 2015, **21**, 5783–5793.

36 K. Ashley, D. B. Parry, J. M. Harris and S. Pons, A conducting polymer formed from the anodic oxidation of toluene in acetonitrile, *J. Chem. Soc., Chem. Commun.*, 1988, 1253–1255.

37 E. Li, G. Shi, X. Hong and P. Wu, Electrochemical polymerization of toluene in the mixed electrolytes of boron trifluoride diethyl etherate and trifluoroacetic acid, *J. Appl. Polym. Sci.*, 2004, **93**, 189–195.

38 B. D. Adamson, S. A. Skeen, M. Ahmed and N. Hansen, Detection of aliphatically bridged multi-core polycyclic aromatic hydrocarbons in sooting flames with atmospheric-sampling high-resolution tandem mass spectrometry, *J. Phys. Chem. A*, 2018, **122**, 9338–9349.

39 S. H. Ng, J. Wang, D. Wexler, S. Y. Chew and H. K. Liu, Amorphous carbon-coated silicon nanocomposites: A low-temperature synthesis via spray pyrolysis and their application as high-capacity anodes for lithium-Ion batteries, *J. Phys. Chem. C*, 2007, **111**, 11131–11138.

40 M. R. Smith, S. W. Hedges, R. LaCount, D. Kern, N. Shah, G. P. Huffman and B. Bockrath, Selective oxidation of single-walled carbon nanotubes using carbon dioxide, *Carbon*, 2003, **41**, 1221–1230.

41 S. Zhang, X. T. Zeng, H. Xie and P. Hing, A phenomenological approach for the Id/Ig ratio and sp^3 fraction of magnetron sputtered a-C films, *Surf. Coat. Technol.*, 2000, **123**, 256–260.

42 A. C. Ferrari, J. Robertson, A. C. Ferrari and J. Robertson, Raman spectroscopy of amorphous, nanostructured, diamond–like carbon, and nanodiamond, *Philos. Trans. R. Soc., A*, 2004, **362**, 2477–2512.
43 M. M. Lucchese, F. Stavale, E. H. M. Ferreira, C. Vilani, M. V. O. Moutinho, R. B. Capaz, C. A. Achete and A. Jorio, Quantifying ion-induced defects and raman relaxation length in graphene, *Carbon*, 2010, **48**, 1592–1597.
44 A. C. Ferrari, Raman spectroscopy of graphene and graphite: Disorder, electron–phonon coupling, doping and nonadiabatic effects, *Solid State Commun.*, 2007, **143**, 47–57.
45 V. L. Kuznetsov, A. L. Chuvilin, Y. V. Butenko, I. Y. Mal'kov and V. M. Titov, Onion-like carbon from ultra-disperse diamond, *Chem. Phys. Lett.*, 1994, **222**, 343–348.
46 J. Yang, Y. Zhang and D. Y. Kim, Electrochemical sensing performance of nanodiamond-derived carbon nano-onions: Comparison with multiwalled carbon nanotubes, graphite nanoflakes, and glassy carbon, *Carbon*, 2016, **98**, 74–82.
47 S. Stankovich, D. A. Dikin, R. D. Piner, K. A. Kohlhaas, A. Kleinhammes, Y. Jia, Y. Wu, S. T. Nguyen and R. S. Ruoff, Synthesis of graphene-based nanosheets via chemical reduction of exfoliated graphite oxide, *Carbon*, 2007, **45**, 1558–1565.
48 L. G. Cançado, A. Jorio, E. H. M. Ferreira, F. Stavale, C. A. Achete, R. B. Capaz, M. V. O. Moutinho, A. Lombardo, T. S. Kulmala and A. C. Ferrari, Quantifying defects in graphene via raman spectroscopy at different excitation energies, *Nano Lett.*, 2011, **11**, 3190–3196.